ENVIRONMENTAL AND GROUNDWATER

*Exploration Geophysics (2001) **32**, 204 - 208*

Detection of cavities and tunnels from gravity data using a neural network

Eslam Elawadi[1] Ahmed Salem[2] Keisuke Ushijima[3]

Key Words: microgravity, cavities, neural network

ABSTRACT

We have developed a simple approach to determine the depth and radius of subsurface cavities from •microgravity data. The horizontal location of cavity centre is picked up as the projection of the minimum of gravity anomaly. Depth to the cavity centre is estimated using a back propagation neural network. The cavity radius can be then calculated using the determined parameters if the density contrast between the host rock and the cavity filling materials is known or assumed according to the geological background. The present method is tested using synthetic data and was able to determine the cavity parameters in the presence of noise. The method was also tested using field data measured over known cavities in the Medford cavity site, Florida USA. The estimated cavity parameters agree with the borehole results. The results show that the method is promising for estimating the parameters of cavities and tunnels from microgravity data.

INTRODUCTION

The detection of natural and artificial cavities is a common task in many scientific and environmental fields such as archaeology and engineering geophysics. In these fields, microgravity surveying (high-precision, high-accuracy, and high-resolution applications of the gravity method) is well suited for the detection and delineation of cavities (Butler, 1977). Examples of the applications of microgravity techniques to the detection of underground cavities are given by Arzi (1975), Butler (1983, 1984), and Fajklewicz (1986).

Natural cavities may be air-filled, water-filled, soft sediment-filled or partially filled with any of the above. For nearly every conceivable situation, the cavity presents a negative density contrast with the surrounding rock. The result is invariably a negative gravity anomaly that can be detected by a sensitive gravity instrument. The interpretation of such an anomaly aims essentially to estimate the cavity parameters such as location, depth, and radius. Several graphical and numerical methods have been developed for interpreting gravity anomalies caused by simple bodies. The simplest formula used to approximate depth to a causative body from the residual gravity data is the half-g_{max} rule (Nettleton, 1942; Telford, 1976). However, the drawback with this approach is that it is highly subjective and can lead to large errors. Gupta (1983) presented a numerical approach to determine the depth to cylindrical and spherical models from the residual gravity data. Abdelrahman (1990) argued that inserting the maximum gravity value g_{max} as a known parameter in Gupta's formulation may lead to large error in the calculation of depth in the existence of noise. Recently, several computer-based methods of inverting gravity data to determine model parameters have been presented with various degrees of success (for example, Li & Oldenburg, 1998; Li & Chouteau, 1998 and Boulanger & Chouteau, 2001). The principal difficulty with the inversion methods is the inherent nonuniqueness of the solution (Li & Oldenburg, 1996). Therefore, there is still a need for an interpretation technique that is robust, rapid, and can provide parameters of the cavities in field situations. One such technique can be found in the emerging field of artificial neural networks.

Artificial neural networks are part of much wider field called artificial intelligence, which can be defined as the study of mental facilities through the use of computational models (Charniak & McDermott, 1985). They have gained popularity in geophysics during the last decade (Van der Baan and Jutten, 2000), because they have shown ability in solving non-linear problems. Moreover, they can reach conclusions from incomplete and noisy data (Spichak and Popova, 2000).

In this paper, we have developed a simple approach to determine cavity parameters from gravity data. First, the horizontal location of the cavity is determined by a moving window seeking the gravity minimum. Then we obtain the depth to the cavity centre using a neural network trained by theoretical gravity signatures of cavities located at different depths. Once the horizontal location and depth are obtained, the radius of the cavity can be calculated if the density contrast between the cavity filling materials and the surrounding rocks can be assumed or estimated through additional measurements. The performance of the method is tested using synthetic data and field examples measured over known cavities.

NEURAL NETWORKS AND BACK PROPAGATION

The study of artificial neural networks were motivated by studies of the neural processes in the brain (Rosenblatt, 1958). These processes encompass computer algorithms that solve several types of problem including classification, parameter estimation, parameter prediction, pattern recognition, completion, association, filtering, and optimisation (Brown & Poulton, 1996).

The artificial neural network is composed of many simple processing elements, which are massively interconnected and operated in parallel. The processing elements, commonly known as neurons, receive the input from and send the output to other processing elements through synaptic connections. Typically, the

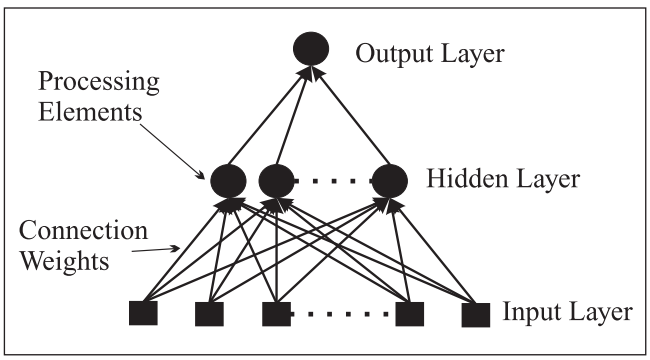

Fig. 1. Schematic representation of a neural network.

Kyushu University, Japan.
[1] *eslam@mine.kyushu-u.ac.jp*
[2] *salem@mine.kyushu-u.ac.jp*
[3] *Ushijima@mine.kyushu-u.ac.jp*

neurons are arranged in layers, i.e., groups of elements, which connect to other layers such that the outputs of one layer provide the input of the next layer. There is a minimum of three layers for nonlinear problems: an input layer, internal or hidden layer, and an output layer (Figure 1).

The neural networks can be divided into two main categories: unsupervised recurrent and supervised feed-forward networks. In the unsupervised recurrent type, the networks allow the information to flow in either direction. These models are called unsupervised because there is no teacher to set up the input/output mapping relation (Salem et al., 2001). In the supervised feed-forward networks, information is only allowed to flow in one direction without back coupling. These nets are supervised because an associated output stimulus is supplied to the network for each input pattern and the connection weights are adapted so that the network learns the desired input/output mapping relation (Poulton et al., 1992).

In this paper, we used the most popular supervised feed-forward network, known as back propagation. The term back propagation refers to the method for computing the error gradient for a feed-forward network, a straightforward but elegant application of the chain rule of elementary calculus (Werbos, 1994). An excellent mathematical discussion of the back propagation neural network can be found in Rumelhart et al. (1986).

THE METHOD

The anomalous gravity effect of cavity targets can be computed directly for idealized geometrical shapes in a homogenous medium (Owen, 1983). For an infinite horizontal cylindrical tunnel, the gravity effect observed along a transverse survey path is

$$\Delta g(x) = \frac{200\pi G\Delta\rho R^2 D}{D^2 + x^2} \qquad (1)$$

and for a spherical cavity, the gravity effect is

$$\Delta g(x) = \frac{400\pi G\Delta\rho R^3 D}{3(D^2 + x^2)^{3/2}} \qquad (2)$$

where G is the gravitational constant ($6.67\text{x}10^{-11}$ NM^2/kg^2), $\Delta\rho$ is density contrast between the cavity filling materials and the host rock (kg/m^3), R is model radius (m), D is the depth to model axis (m), and $\boldsymbol{x}$ is the instrument offset distance from the cylinder axis or the sphere centre (m). In equations (1) and (2), Δg ($\boldsymbol{x}$) attains minimum at $\boldsymbol{x} = 0$ i.e., the horizontal location of the cavity centre ($\boldsymbol{x}_0$) can be obtained as the projection of the gravity anomaly minimum.

The back propagation neural network is used to obtain the depth to the cavity centre at the location yielding the minimum gravity response. For this purpose, a network of three layers was designed with 21 neurons in the input layer (representing the input measurements); five neurons in the hidden layer; and one output neuron (representing the depth to the cavity). Prior to training the network, the input gravity data and the corresponding depth were scaled in the range of (0,1). Scaling the output data is essential for a neural network to be able to properly learn from the training examples. On the other hand, scaling the input data to a small range usually improves the performance of the network by minimizing the chance of saturation due to large input values. The network was trained by a set of 15 synthetic examples, for each cylindrical and spherical cavity models, located at depths between 1 and 8 m. Figure 2 shows the network error versus the iteration number during the learning for the cylindrical and spherical cavity examples. The network attained the convergence after about 13000 iterations in 6 minutes, for each model, using a Pentium II 233 computer.

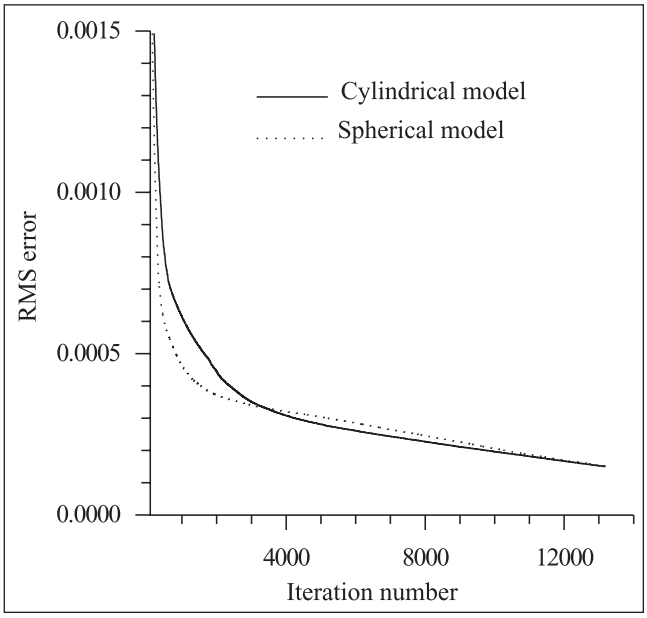

Fig. 2. RMS error as a function of iteration number during learning by the network for cylindrical models (solid) and spherical models (dotted).

The performance of the trained network was tested using synthetic gravity data for both cylindrical and spherical models. The testing sets contain gravity signatures of 14 cavity models located at different depths from those on which the network was trained. The network showed a potential to estimate the depth of the testing examples with maximum relative error of 0.8% and 0.6% for the cylindrical and spherical cavity models, respectively (Figure 3).

Up to this stage, we have determined the cavity location and depth ($\boldsymbol{x}_0$ and D). Using these parameters, the radius for cylindrical and spherical models can be directly calculated from equations (1) and (2) if the density contrast ($\Delta\rho$) between the cavity filling material and the surrounding host rock is available or can be determined through additional measurements.

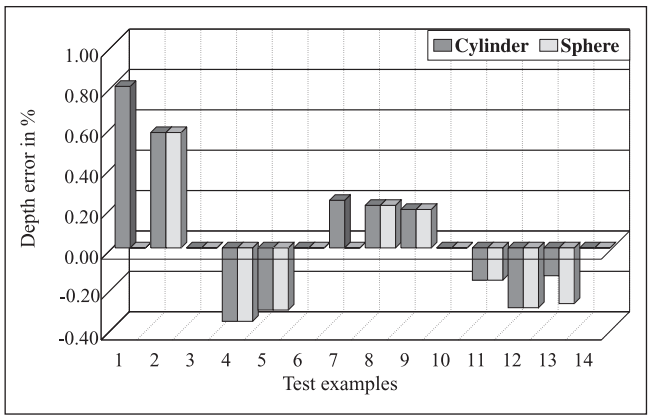

Fig. 3. Depth error, in percent, for the cylindrical and spherical test examples.

SYNTHETIC EXAMPLES

The performance of the method has been tested by different sets of synthetic gravity data for both cylindrical and spherical cavity models. The object of these tests is to evaluate the sensitivity of the method to natural noise as well as different sources of errors.

Effect of random noise

Variation in subsurface geology and surface topographical relief can introduce noise in the gravity measurements that may affect or disfigure the anomaly produced by the cavity target. Therefore, it is important to investigate the noise influence in the efficiency of the present method. To achieve this, the gravity response over cylindrical and spherical cavity models of 1.0 m radius and

Random noise to signal ratio(%)	Cylinder		Sphere	
	Depth error (%)	Radius error (%)	Depth error (%)	Radius error (%)
0	0.2	1.6	0.2	1.6
2	2.6	1.8	2.2	2.1
4	4.8	2.1	4.1	2.7
6	6.6	2.3	6.8	3.3
8	8.6	2.6	7.4	3.9
10	11.2	2.9	8.1	4.5

Table 1. Calculated depth and radius error, in percent, for cylindrical and spherical models imposed by random noise.

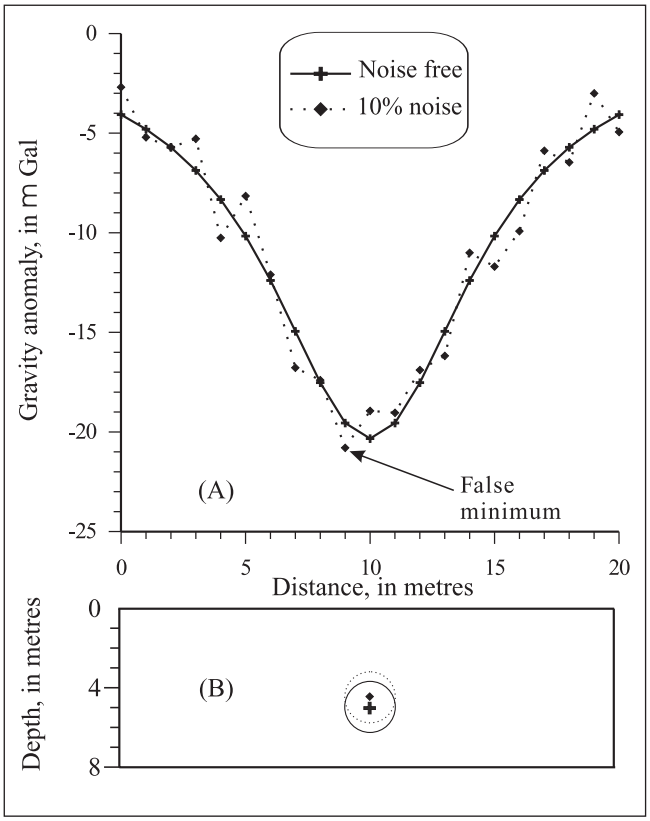

Fig. 4 (A). 2-D gravity anomaly due to a cylindrical model of 1.0 m radius, -2.5 kg/m³ density contrast, buried at 5.0 m depth (solid); with the same data imposed by 10% random noise (dotted). (B) Cylindrical model interpreted from the noisy data (dotted) in comparison with the original model (solid).

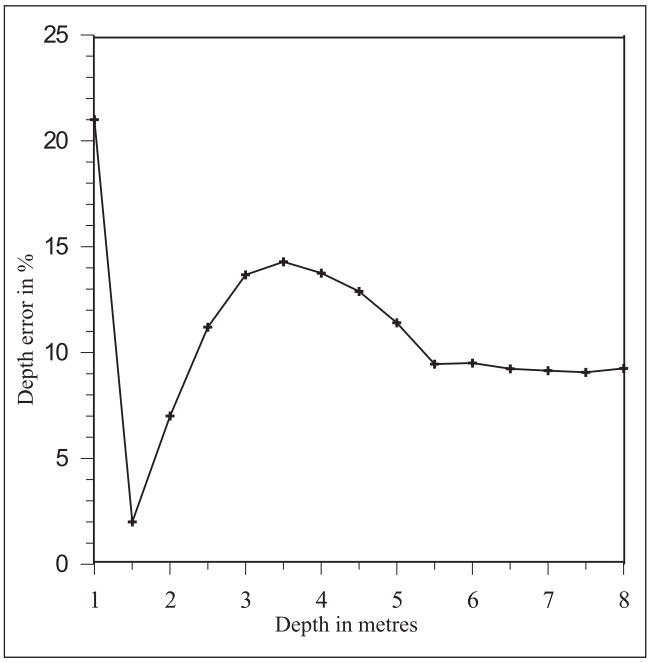

Fig. 5. Relative depth error due to a one-metre shift of x_0 produced by 10% noise, for a cylindrical model located at depths from 1 to 8 m.

-2.5x10³ kg/m³ density contrast, buried at 5 m depth were calculated and contaminated by random noise with amplitudes representing 0 to 10% of the maximum anomaly value (Figure 4A). Applying the method to the noisy data, the errors in the depth and radius increase proportionally with the noise ratio. The depth error ranges from 0.2 to 11.2% for the cylindrical model, and from 0.2 to 8.1% for the spherical model (Table 1& Figure 4B). Meanwhile, the percentage of error in the radius ranges from 1.6% to 2.9% and from 1.6% to 4.5% for the cylindrical and spherical models, respectively.

As noted, this method begins with obtaining the location of cavity centre as the projection of the gravity anomaly minimum (x_0). Moreover, the neural network is trained with the assumption that the model centre, coincident with the minimum value, is located at the centre of the profile. As shown in Figure 4(A), the location of the minimum value (x_0) may be shifted from the actual location due to the natural noise. This may lead to errors in the estimated depth. To understand the effect of such error, the method was tested with a set of synthetic data in which the minimum value is shifted one metre before the profile centre due to 10% noise. Figure 5, shows the error in the depth obtained for these examples. The estimated depth for the model located at depth of one metre (equal to the shift in x_0) is highly affected by the shift. Except in this example, the errors in the estimated depths ranged from 2 to 14.3%. This indicates that the method gives reasonable depth even when the horizontal location of the body is approximately determined.

To ascertain the errors in the calculation of the radius due to inaccuracies in the density contrast, we simulated the expected errors from equations 1 and 2 using values of density contrast that under and overestimated the correct value by 20% (Figure 6). As a result, the error in the calculated radius ranged from 12 to -8% and from 7.5 to -5% for the cylindrical and spherical models respectively. Generally, the error in the assumed density contrast produces a much lower error in the calculated radius for the models under consideration.

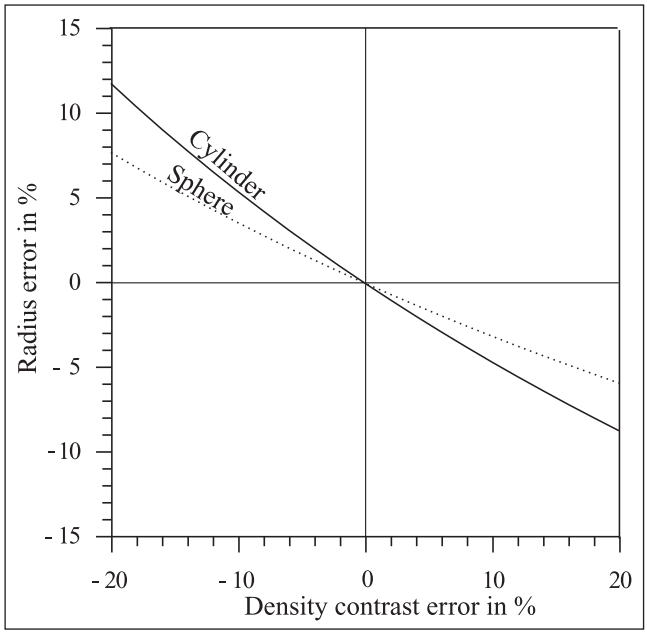

Fig. 6. Error response in radius versus percentage error imposed in the density contrast of the cylindrical and spherical cavity models.

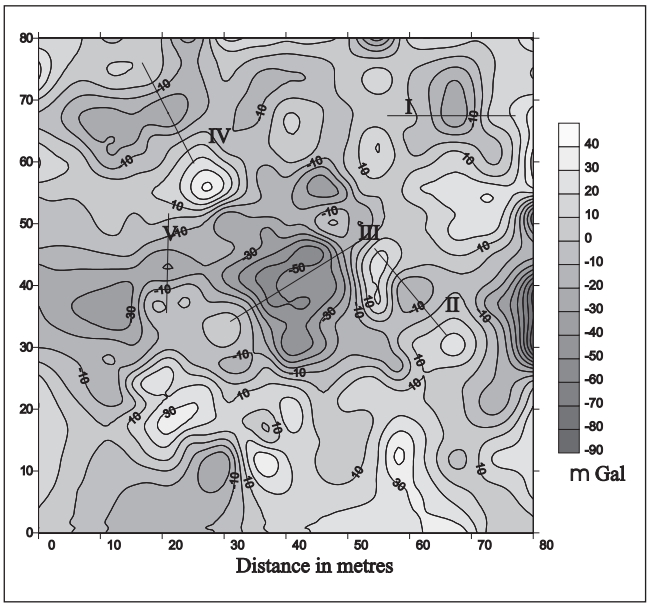

Fig. 7. Residual gravity anomaly map for the Medford cave site (Butler, 1983), showing the location of five profiles selected as test examples.

FIELD EXAMPLE

We used field microgravity data measured over known cavities at the Medford cave site, Florida UAS, to test the efficiency of the method in practical situations. The microgravity survey of the Medford cave site utilized a LaCost-Romberg model D-4 gravimeter, with about 1 μ Gal sensitivity, to obtain 420 readings over an approximately 80 m by 80 m area (Butler, 1983 & 1984). A basic grid dimension of 6.1 m (20 ft) was used, with a 3 m (10 ft) grid used in the central portion of the area over the known cavity system. Standard tidal and drift corrections were applied to the data, as were Bouguer and terrain corrections. A planar regional field was determined by inspection and removed (Butler, 1983) to produce a residual gravity anomaly map (Figure 7). We selected five profiles (labelled I to V) to test the method, each containing 21 observations interpolated at 1 m interval. The gravity data were scaled and assigned to the output of the processing elements of the input layer. Using the previously adapted set of weights for the sphere and cylinder models, the network estimated the depths for each profile. Using these depths and the average density measured at the nearest borehole to each profile, the radii for the assumed models were calculated.

To compare the interpreted parameters with the borehole results, the interpreted cavities parameters were transformed to depths to top and depths to bottom (Tables 2a and 2b). Except for the profile III, the results of the method are in agreement with the drilling information; taking into account the differences between the assumed simple models and the actual cavity system, which is more complicated. Assuming a cylindrical target, the interpreted depths to the top agree to better than 23% and the depths to the bottom to better than 24% of the known cavity dimensions. Assuming a spherical target, the errors in the interpreted depths to the tops and bottoms increased to 28% and 51%, respectively. The significant error in the interpreted depths from profile III is most probably due to interference in the observed data because of multiple cavity features located at close depths as shown by drilling (Table 2a).

The performance of the method was also investigated by comparing the results with those attained by a least square method (Gupta, 1983) for the same field examples. In Gupta's method, the problem of depth determination of buried structure from the residual gravity anomaly has been transformed into a problem of finding the solution of a non-linear equation of the form $f(z) = 0$. Comparing the results (Tables 2a and 2b) reveals that both methods provide reliable solutions. However, the results of our method are much closer to the borehole information for most of the anomalies (I, IV and V, assuming a cylindrical model and I, II, IV and V, assuming a spherical model). On the other hand, the results of Gupta's method are better for the rest of the anomalies (II, III, assuming a cylindrical model and III, assuming a spherical model). This indicates that the present method is an effective tool for the detection of cavities from gravity anomaly data. However, the accuracy of the results depends on precise separation of residual gravity anomalies from the regional field. To make the application of the method more relevant, we are exploring the use of gradient measurements.

CONCLUSIONS

In this paper, we developed a simple approach to determine the location and radius of cavities and tunnels from microgravity anomaly data. The horizontal location is determined as the projection of the minimum value of the gravity anomaly. The depth is estimated using a trained back propagation neural network. The radius is then calculated using the estimated parameters and the density contrast between the host rock and the cavity filling materials.

The present approach is tested using synthetic data for spherical and cylindrical models. The errors in the estimated depths are less than 0.8% for both models. After adding random noise up to ± 10% to the synthetic data, the depths obtained are within ± 11.2% for the cylindrical models and ± 8.1% for the spherical models. The approach was also tested using field microgravity data measured above known cavities at the Medford cave site, Florida, USA. Generally, the estimated cavity parameters agree well with the parameters proved by drilling. We conclude that the present method can provide fast and robust determination of cavity parameters in the field situation.

Anomaly Number	Borehole Results		Results of the present method		Results of Gupta's method	
	Depth (m) To		Depth (m) To		Depth (m) To	
	Top	Bottom	Top	Bottom	Top	Bottom
I	2.74	4.41	2.60	5.20	1.83	5.17
II	2.74	5.48	2.09	4.21	2.36	5.04
III	4.57	7.92	2.35	6.11	3.00	8.00
*	8.68	9.29				
IV	3.90	7.80	3.04	5.90	1.73	4.27
V	2.71	5.42	2.88	6.04	2.86	7.14

* Two levels of cavities encountered at this location.

Table 2a. Interpreted cavity parameters (suggesting a cylindrical target) for the selected profiles of the Medford cavity site, in comparison with the borehole results and the results obtained by the least square method.

Anomaly Number	Borehole Results		Results of the present method		Results of Gupta's method	
	Depth (m) To		Depth (m) To		Depth (m) To	
	Top	Bottom	Top	Bottom	Top	Bottom
I	2.74	4.41	2.26	7.06	2.10	7.10
II	2.74	5.48	1.96	5.76	2.30	7.70
III	4.57	7.92	1.99	8.39	3.40	12.6
*	8.68	9.29				
IV	3.90	7.80	2.86	8.16	2.62	8.42
V	2.71	5.42	2.42	8.22	3.21	8.41

* Two levels of cavities encountered at this location.

Table 2b. Interpreted cavity parameters (suggesting a spherical target) for the selected profiles of the Medford cavity site, in comparison with the borehole results and the results obtained by the least square method.

ACKNOWLEDGEMENTS

We express our appreciation to D.K. Butler for granting permission to use the Medford site gravity data. Also we would like to extend our thanks to all the staff of the Exploration Geophysical Lab in Kyushu University for their contribution and support during this work. Finally, we sincerely acknowledge the Associated Editor and the anonymous reviewers for valuable and constructive comments, which greatly improved the manuscript.

REFERENCES

Abdelrahman, E. M., 1990, Discussion on "A least-squares approach to depth determination from gravity data" by O.P. Gupta: Geophysics, **55**, 376-378.

Arzi, A. A. 1975, Microgravity for engineering applications: Geophs. Prosp., **23** 408-425.

Boulanger, O. and Chouteau, M., 2001, Constraints in 3D gravity inversion, Geophysical Prospecting, **49**, 265-280.

Brown, M. P. and Poulton, M. M., 1996, Locating buried objects for environmental site investigations using Neural Networks: JEEG, **1**, 179-188.

Butler, D.K., Ed. 1977, Proc. of the symposium on detection of subsurface cavities: U.S Army Engineer Waterways Experiment Station, CE, Vicksburg, MS.

Butler, D.K., 1983, Cavity detection research, Report 1, Microgravimetric and magnetic surveys, Medford Cave Site, Florida: Tech. Rep.GL-83-1, U.S Army Engineer Waterways Experiment Station, CE, Vicksburg, MS.

Butler, D.K., 1984, Microgravimetric and gravity gradient techniques for detection of subsurface cavities: Geophysics, **49**, 1084-1096.

Charniak E. and McDermott D., 1985, Introduction to Artificial Intelligence, Addison-Wesley.

Fajklewicz, Z., 1986., Origin of the anomalies of gravity and its vertical gradient over cavities in brittle rock: Gophys. Prosp., **4(8)**, 1233-1254.

Gupta, O. P., 1983, A least-squares approach to depth determination from gravity data: Geophysics, **48**, 537-360.

Li, X., and Chouteau, M., 1998, Three-dimensional gravity modelling in all space, Surveys in Geophysics, **19**, 339-368.

Li, Y., and Oldenburg, D.W., 1996, 3-D inversion of magnetic data: Geophysics, **61**, 394-408.

Li, Y., and Oldenburg, D.W., 1998, 3-D inversion of gravity data: Geophysics, **63**, 109-119.

Nettleton, L. L., 1942, Gravity and magnetic calculation: Geophysics, **7**, 293-310.

Owen, T. E., 1983, Detection and mapping of tunnels and caves: Developments, in Geophysical Exploration Methods, A. A. Fitch (ed.), Vol. **5**, 161-258 Applied Science Publishers Ltd.

Poulton, M.M., Sternberg, B.K., and Glass, C.E., 1992, Location of subsurface targets in geophysical data using neural networks, Geophysics, **57**, 1534-1544.

Rosenblatt. F.,1958, The perceptron: A probabilistic model for information storage and organization in the brain: Psychological Review, **65**, 386-408.

Rumelhart, D.E., Hinton, G.E., and Williams, R.J., 1986: Learning internal representations by error propagation, in Rumelhart, D. E., and McClelland, J. L., Eds., Parallel distributed processing: Explorations in the Microstructure of Cognition, **v.1**, p.318-362, Cambridge, MA: The MIT Press.

Salem, A., Ravat, D., and Ushijima, K.,2001, Subsurface imaging of buried steel drums from magnetic data using Hopfield neural network, Proc. of the 5th SEGJ International Symposium, Tokyo, 369-375.

Spichake, V., and Popova, I., 2000, Artificial neural network in inversion of magnetotelluric data in terms of three-dimensional earth macroparameters: Geophys. J. Intl., **142**, 15-26.

Telford, W. M., Geldart, L. P., Sheriff, R. E., and Key, D. A., 1976, Applied Geophysics: London, Cambridge Univ. Press.

Van der Baan, M., and Jutten, C., 2000, Neural networks in geophysics: Geophysics, **65**, 1032-1047.

Werbos, P.J., 1994, The roots of back propagation, NY: John Wiley & Sons.